

## The Changing Character of Carbon in Fluids with Pressure: Organic Geochemistry of Earth's Upper Mantle Fluids

Dimitri Sverjensky<sup>1</sup>, Isabelle Daniel<sup>2</sup>, and Alberto Vitale Brovarone<sup>3,4</sup>

### ABSTRACT

Decades of research have now firmly established that aqueous fluids in Earth's crust from groundwater to deep basinal brines to shallow mid-ocean ridge hydrothermal systems can contain metastable equilibria involving C-species in which methane does not participate. It now appears, however, that this situation does not extend to the upper mantle. Instead, field evidence from theoretical models, experimental diamond-anvil cell and fluid inclusion studies, and high-pressure metamorphic rocks all indicate a wide variety of aqueous C-species at high pressures. At pressures above about 2.0–3.0 GPa, methane and all other aqueous C-species with different oxidation states between -4.0 and +4.0 can coexist in variable proportions. Furthermore, the aqueous fluids can coexist with immiscible hydrocarbon fluids. As a consequence, C-species with a mixture of oxidation states in aqueous fluids and hydrocarbon fluids at high pressures in the upper mantle can influence the oxidation state of their upper mantle environment.

### 22.1. INTRODUCTION

A wide variety of aqueous carbon species occurs in fluids located at the surface of Earth to at least upper mantle depths. Interestingly, however, the modeling treatment of aqueous carbon species tends to depend on the geochemical environment in which they are found. For example, in seawater, aqueous inorganic carbon speciation has been treated using the classical inorganic C-species  $\text{CO}_2$ ,  $\text{HCO}_3^-$ , and  $\text{CO}_3^{2-}$ , and Ca and Mg complexes of the ions. Such models have been very thoroughly

studied under surficial conditions, where their relative abundances generally reflect thermodynamic equilibria and are crucial to an understanding of seawater chemistry, life in the oceans, and therefore climate change. The same species in various proportions are important in rainwater, soil water, and shallow groundwaters, together with a wide range of organic C-species that are completely out of thermodynamic equilibrium with the inorganic species. However, in deep groundwaters, such as those in sedimentary basins where sampled fluids reach temperatures on the order of 150 °C, some aqueous organic carbon species (e.g.  $\text{CH}_3\text{COO}^-$ ) are in chemical communication with the inorganic ones, forming metastable thermodynamic equilibria, as will be discussed below (Shock, 1988, 1990). At the even higher temperatures of hot-spring and mid-ocean ridge environments (up to about 400 °C), a wide array of metastable equilibria may exist (Manning et al., 2013; McCollom, 2013).

In contrast, in crustal metamorphic environments at temperatures much greater than 400 °C, a very different treatment of aqueous carbon speciation has prevailed.

<sup>1</sup> Department of Earth and Planetary Sciences, Johns Hopkins University, Baltimore, Maryland, USA

<sup>2</sup> Université Lyon, Université Lyon 1, Ens de Lyon, CNRS, UMR 5276, Laboratoire de Géologie de Lyon, Villeurbanne, France

<sup>3</sup> Dipartimento di Scienze della Terra, Università degli studi di Torino, Torino, Italy

<sup>4</sup> Sorbonne Université, Museum National d'Histoire Naturelle, UMR CNRS 7590, IRD, Institut de Minéralogie, des Physique de Matériaux et de Cosmochimie, Paris, France

Crustal metamorphic fluids have long been generally treated as simple molecular mixtures, e.g.  $\text{CO}_2$ ,  $\text{CO}$ ,  $\text{CH}_4$ ,  $\text{H}_2$ , and  $\text{H}_2\text{O}$ . For simplicity, models of the fluids are often referred to as COH fluids (Zhang & Duan, 2009). Three assumptions are inherent in COH fluid models. First, the fluids are assumed to contain no other solutes, e.g. no Na, K, Mg, Fe, Ca, Al, or Si, even though they are generally regarded as being in equilibrium with their host rocks and every mineral in the rocks has a definite solubility under these conditions. Second, only molecular species such as those listed above are in the model fluids. There are no ions. As a consequence, there can be no concept of pH, which is such an important parameter in the near-surface environment. Third, the fugacity of oxygen is the only chemical link between the fluids and rocks, except for the molecules listed above, typically  $\text{CO}_2$ ,  $\text{CH}_4$ , and  $\text{H}_2\text{O}$ . The same overall approach has been widely used for fluids in subduction zones, even though decades of experimental studies have shown that at temperatures of about 700 °C to 1,200 °C and pressures approaching 2.0 GPa, the solubilities of minerals in aqueous fluids become substantial (Manning, 2004; Manning, 2018).

In upper mantle environments such as the subcratonic lithospheric mantle, at temperatures of about 800 °C–1,400 °C and pressures of about 4.0 to 6.0 GPa, the COH fluid model has again been the default model for aqueous C-species in the deep Earth. However, fluid inclusion and experimental studies have demonstrated the importance of much higher solute concentrations in the fluids than even in crustal metamorphic environments. Models of the C-speciation vary from high-pressure extensions of the COH fluid model to discussions of a class of fluids termed high-density fluids, or HDFs (Navon, 1999), which are often equated with melts. Such models are very constrained in their ability to explain the causes of diamond formation and how the fluids may also be involved in mantle metasomatic processes that influence the geochemical and mineralogical evolution of the subcratonic lithospheric mantle. The reason is that the COH fluid models have relied almost entirely on invoking redox changes as the cause of precipitation of diamond. In fact, either oxidation of  $\text{CH}_4$  or reduction of  $\text{CO}_2$  to form diamond are the only chemical processes that can be invoked using a COH fluid model. The HDF model relies more on inferring potential processes by using trace element and isotopic tracers as proxies for fluid and/or melt interaction with upper mantle rocks.

Recent developments in theoretical and experimental aqueous geochemistry enable a new treatment of aqueous C-speciation in deep crustal and upper mantle fluids that is analogous to the classical models of surficial and shallow crustal fluids. A continuous modeling capability from surficial to upper mantle conditions is now possible with the Deep Earth Water (DEW) model (Sverjensky,

Harrison, et al., 2014; Huang & Sverjensky, 2019). Predictive speciation models of subcratonic lithospheric mantle fluids involving aqueous ions and metal complexes have been developed (Huang et al., 2017; Mikhail et al., 2017; Mikhail & Sverjensky, 2014; Sverjensky, Harrison, et al., 2014; Sverjensky, Stagno, et al., 2014) based on Raman spectroscopic data for C-bearing ions (Facq et al., 2016; Facq et al., 2014), ab initio theoretical results (Pan & Galli, 2016; Pan et al., 2013), and measured mineral solubilities (Manning, 1994; Tropper & Manning, 2007). The fundamental model does not change from shallow to deep conditions in the Earth. In contrast to the COH and HDF models, the DEW model enables examination of changes in equilibrium aqueous speciation from surficial to deep Earth conditions, and treats a much greater variety of species, including ions and metal complexes. As a result, it is possible to examine patterns of change in aqueous fluid speciation from shallow to deep conditions in a way that was not previously possible.

As an example of recent advances in the modeling of deep Earth fluids, it has been predicted that aqueous inorganic and organic C-species can be in complete thermodynamic equilibrium in deep Earth fluids, in marked contrast to geochemical systems at lower temperatures (Sverjensky, Stagno, et al., 2014). Furthermore, recent ab initio calculations of speciation in aqueous fluids have demonstrated that under upper mantle temperatures and pressures, new species become important. At 1,000 K and 10.0 GPa, ab initio and thermodynamic calculations show that  $\text{CO}_2^0$  is not an important species. Instead,  $\text{H}_2\text{CO}_3^0$  is the major oxidized neutral carbon species (Pan & Galli, 2016). This is a major difference to the traditional COH fluid model for metamorphic and deep Earth fluids. Experimental studies have also indicated changes in the character of aqueous C-species at elevated pressures. Aqueous methane forms rapidly and easily at high pressures (Huang et al., 2017; Scott et al., 2004) and immiscible aliphatic hydrocarbon fluids coexisting with oxidized species of carbon have been documented (Li, 2017; Huang et al., 2017). Together, these advances in theory and experiments represent a first step towards understanding the potential role of aqueous C-species during fluid-rock interactions in the deep Earth.

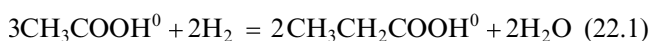
Recent field discoveries have also indicated marked differences in the behavior of C-species between conditions in the mid-ocean ridge hydrothermal systems and those in subduction zones at upper mantle conditions. The amounts of aqueous methane in mid-ocean ridge hydrothermal systems are small. They may be of biologic origin, or inherited from preexisting fluid inclusions in minerals in the igneous oceanic crust (McDermott et al., 2015), or related to catalysis by chromitite minerals (Etiope et al., 2018). In contrast, abundant immiscible abiotic methane has now been documented in alpine

ultramafic massifs previously equilibrated at upper mantle pressures (Vitale Brovarone et al., 2017). The effects of hydrocarbon immiscibility on the mobility and reactivity of deep carbon remain poorly constrained. Hydrocarbon immiscibility phenomena likely affect the wettability of porous media at depth, and thereby the mobility of deep carbon. This feature can potentially lead to unexpected reactivity of mineral surfaces and localized-fluid-rock equilibria.

In the present study, we wish to draw attention to evidence for the changing character of aqueous C-species with temperature and pressure. Based on the discussion above, two major regimes with very different behavior of carbon species are now clear. Aqueous C-species appear to behave completely differently in the shallow crustal environments compared with the upper mantle. In order to emphasize the transition between the two environments, we summarize below the key evidence for these two major regimes.

## 22.2. CARBON SPECIATION IN SHALLOW CRUSTAL FLUIDS

Long-term metastability of aqueous C-species on geologic timescales was first proposed decades ago based on theoretical interpretation of the measured abundances of short-chain aliphatic acids in oil-field brines (Shock, 1988). As an example, it can be seen in Figure 22.1a that Gulf Coast brines systematically cluster about a line with a theoretical slope of 1.5 consistent with the equilibrium



and a rearrangement of the corresponding Law of Mass Action represented by

$$\log a_{\text{CH}_3\text{CH}_2\text{COOH}^0} = +1.5 \log a_{\text{CH}_3\text{COOH}^0} + (0.5 \log K - 2 \log f_{\text{H}_2}) \quad (22.2)$$

The correlation strongly suggests that there is an equilibrium between the organic acid anions.

The intercepts of the lines defined by equation (22.2), together with theoretically calculated values of  $\log K$ , enable calculation of values of  $f_{\text{H}_2}$  for the oil field brines. The values of  $\log f_{\text{H}_2}$  are shown by the symbols in Figure 22.1b. The contours on the plot represent theoretically calculated values of  $\log f_{\text{CO}_2}$  calculated from the hypothetical equilibrium



Values of  $\log f_{\text{CH}_4}$  were calculated from another hypothetical equilibrium:



The hatched area in Figure 22.1b is limited by an upper value of  $f_{\text{CO}_2}$  equal to less than the total pressure in the system. It can be seen that the symbols in Figure 22.1b clearly overlap with the  $\log f_{\text{CO}_2}$  values, i.e. the calculated  $f_{\text{H}_2}$  values of the brines are consistent with  $f_{\text{CO}_2}$  values less than the total pressure. However, corresponding values of the calculated  $f_{\text{H}_2}$  values of the brines are not consistent

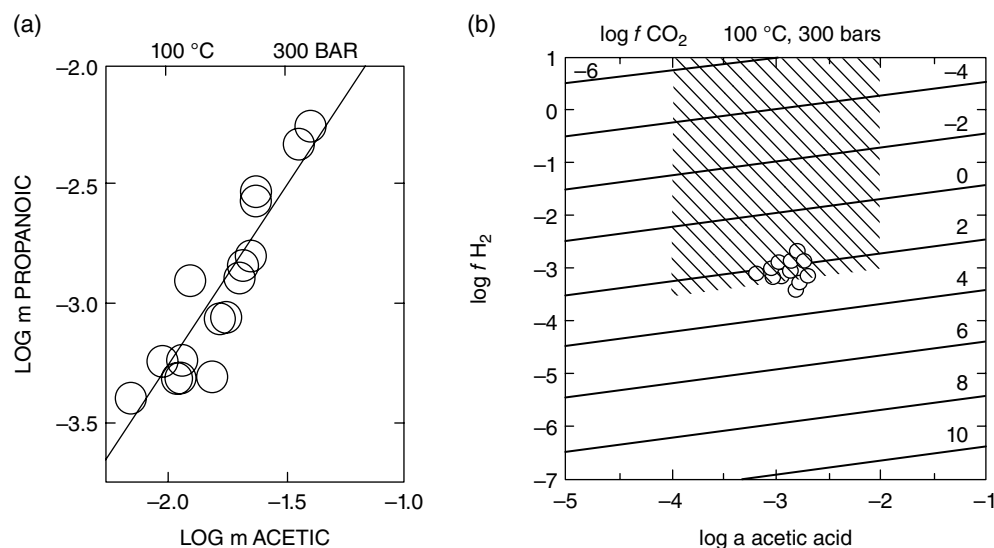
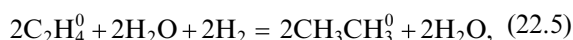


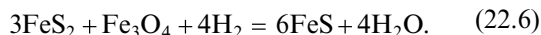
**Figure 22.1** Metastable equilibria in oil-field brines (Shock, 1988, 1990). (a) Logarithms of the molalities of aliphatic acids in oil-field brines relative to a line with a theoretical slope of 1.5. (b) Values of the logarithm of the hydrogen gas fugacity for oil-field brines such as those defined by (a) and their acetic acid concentrations. The contours represent the hypothetical fugacity of CO<sub>2</sub> in metastable equilibrium with the acetic acid. See electronic version for color representation of the figures in this book.

with  $f_{\text{CH}_4}$  values less than the total pressure. Instead, they suggest hypothetical  $f_{\text{CH}_4}$  values on the order of 10,000 bars, which is completely unreasonable. Overall, Figures 22.1 a and b strongly suggest that a metastable equilibrium between aliphatic acids and  $\text{CO}_2$  is possible, but that  $\text{CH}_4$  is out of equilibrium with the other carbon-bearing species.

Subsequent experimental studies have confirmed the validity of the concept of metastable equilibrium between aqueous C-species when methane is kinetically hindered from reacting under shallow crustal conditions. The first example involved the demonstration of equilibrium at 325 °C and 350 bars between ethene and ethane (Seewald, 1994), which can be written



with  $f_{\text{H}_2}$  buffered by the mineral assemblage pyrite-pyrrhotite-magnetite according to the equilibrium



Over a period of hundreds of hours, a steady state of the aqueous species was reached that is well within uncertainties of the predicted thermodynamic metastable equilibrium. Numerous subsequent studies have confirmed reversible hydrothermal metastable equilibria among many types of aqueous organic species (McCollom & Seewald, 2003a, 2003b; Seewald et al., 2006), including aromatic aqueous C-species (Shipp et al., 2013; Shock et al., 2013; Yang et al., 2012).

Confirmation of the existence of metastable equilibria in the field has been more elusive (Etiope & Sherwood Lollar, 2013). The outstanding example remains that of oil-field brines discussed above. Numerous studies have suggested that small amounts of methane in mid-ocean ridge systems have been formed by abiotic synthesis facilitated by mineral catalysis. But this is difficult to demonstrate beyond reasonable doubt. Other studies have suggested that methane in gas seeps and springs associated with ultramafic bodies has an abiotic origin catalyzed by Cr or Ru in rocks (Etiope et al., 2018). The strongest evidence of a metastable equilibrium is the recent study of serpentine in the mid-ocean ridge Atlantis Massif. The study demonstrated that the amino acid tryptophan formed from a natural abiotic synthesis catalyzed by iron-rich clay minerals (Ménez et al., 2018). This remarkable discovery has wide-ranging implications for the metastable organic geochemistry of mid-ocean ridge hydrothermal systems, as the formation of amino acids and other biomolecules has long been predicted theoretically. Interestingly, tryptophan had previously been predicted

to be one of the two most likely amino acids to occur by abiotic synthesis in a wide range of mid-ocean ridge hydrothermal systems (Shock & Canovas, 2010). Figures 22.2 a and b show predictions of the chemical affinity for tryptophan or phenylalanine to form during mixing of many different mid-ocean ridge hydrothermal fluids with cold seawater under conditions of metastable equilibrium. The very large positive chemical affinities indicate a strong thermodynamic driving force favoring the formation of the organic molecule in each case in the absence of methane. This prediction agrees well with the Atlantis Massif discovery of abiotic tryptophan.

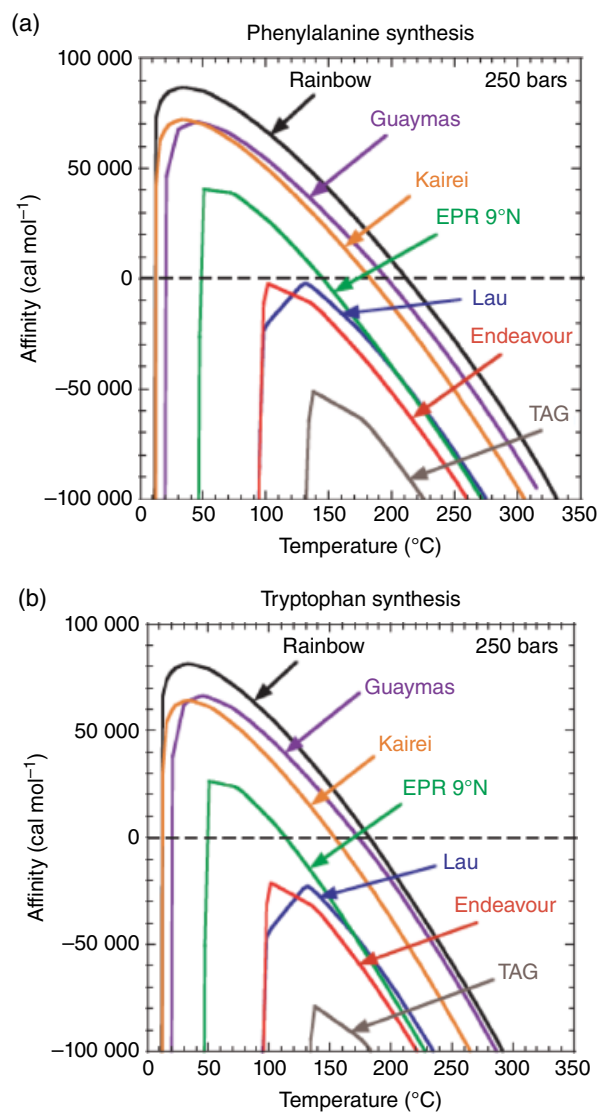


**Figure 22.2** Predicted thermodynamic driving force (affinity) for amino acid synthesis in mid-ocean ridge fluids mixing with ambient seawater (Shock & Canovas, 2010). (a) Phenylalanine. (b) Tryptophan. See electronic version for color representation of the figures in this book.

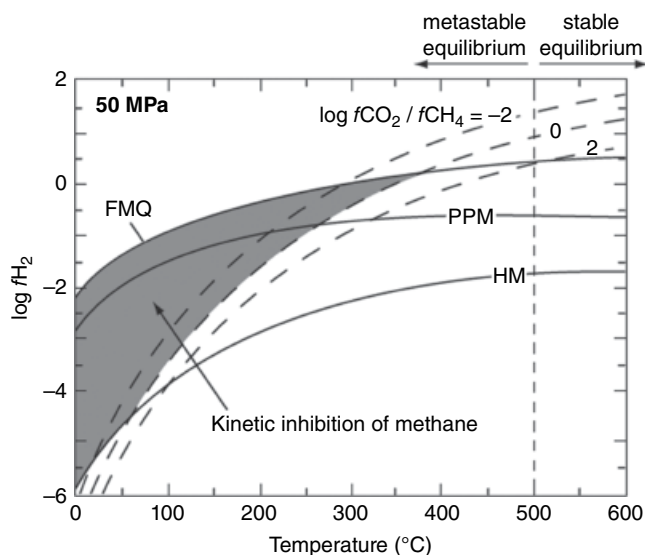


**Figure 22.3** Prediction of the conditions of metastable equilibria under shallow crustal conditions where methane formation is kinetically inhibited (shaded area) (Manning et al., 2013) and metastable equilibria of other C-bearing species is favored. Solid curves represent mineral hydrogen buffers and dashed curves represent contours of the fugacity ratio of  $\text{CO}_2$  and  $\text{CH}_4$  gases. See electronic version for color representation of the figures in this book.

Overall, the kinetic reluctance of aqueous methane to participate in reactions with other aqueous C-species opens up the possibility of a rich set of metastable equilibria between C-bearing species in crustal hydrothermal systems (Figure 22.3). The solid curves in the figure refer to the mineral reactions that might buffer the fugacity of  $\text{H}_2$ . The potential range of conditions under which metastable equilibria are most likely to be detected is summarized by the shaded area in Figure 22.3 (Manning et al., 2013, after Shock, 1992), i.e. at temperatures less than about 400 °C. It is at these temperatures that the kinetics of formation of  $\text{CH}_4$  are expected to be so slow that natural fluids in the shallow crust will contain a wide variety of aqueous organic carbon species in metastable equilibrium with  $\text{CO}_2$ ,  $\text{HCO}_3^-$ , and  $\text{CO}_3^{2-}$ , as well as carbonate minerals. The likely upper temperature limit for metastable equilibria is suggested to be about 500 °C. Above this temperature, it is suggested that the kinetics of reversible reduction of  $\text{CO}_2$  to  $\text{CH}_4$  are sufficiently fast that a full thermodynamic equilibrium in aqueous solution will exist. Such fluids should contain  $\text{CO}_2$ ,  $\text{CH}_4$ ,  $\text{HCO}_3^-$ ,  $\text{CO}_3^{2-}$ , and related metal complexes of the ions. They should not contain other aqueous organic species in any significant concentrations (Manning et al., 2013). It should be emphasized that Figure 22.3 refers to a pressure of 50 bars. However, as will be discussed below, at much higher

pressures, it is possible that a completely different situation exists.

## 22.3. CARBON SPECIATION IN UPPER MANTLE FLUIDS

### 22.3.1. Theoretical Studies

#### 22.3.1.1. The End of Metastability: The Aqueous Organic Geochemistry of the Upper Mantle

The COH fluid model has been widely used to address the expected species of aqueous carbon under upper mantle conditions. As an example, calculated variations in the mole fractions of  $\text{CO}_2$  and  $\text{CH}_4$  in fluids in equilibrium with graphite or diamond as a function of depth in the Earth (Zhang & Duan, 2009) only include these species and  $\text{H}_2\text{O}$ ,  $\text{CO}$ ,  $\text{H}_2$ , and  $\text{C}_2\text{H}_6$ . There are no ions. It is assumed that the  $f_{\text{O}_2}$  is imposed exclusively by the intramineral equilibrium in rocks sampled as xenoliths from the subcratonic lithospheric mantle. Between depths of about 100 and 200 km,  $\text{H}_2\text{O}$ -rich fluids are predicted to transition from having  $\text{CO}_2$  as the predominant C-species to  $\text{CH}_4$  as the main C-species (Zhang & Duan, 2009). In other words, the transition between about 100 and 200 km is from fluids with high  $\text{CO}_2/\text{CH}_4$  ratios to fluids with high  $\text{CH}_4/\text{CO}_2$  ratios. This conclusion about C-speciation in upper mantle fluids is widely used in discussions of diamond formation (Shirey et al., 2013). The simplicity of the COH model for C-speciation at upper mantle conditions stands in contrast to the complexity of metastable C-speciation possible below about 500 °C under shallow crustal conditions indicated by Figure 22.3 and the crustal oil-field type brines discussed earlier. The contrast has traditionally been taken to indicate that at shallow crustal conditions metastability prevails, with many different aqueous C-species with different oxidation states, but that at upper mantle conditions a simple equilibrium C-speciation exists, with the two main oxidation states of C, i.e.  $\text{CH}_4$  and  $\text{CO}_2$ , and not much in between. This situation persisted for decades until it became possible to use a different model for upper mantle fluids.

At crustal pressures and at temperatures greater than about 500 °C, under which  $\text{CH}_4$  can be assumed to freely react, the expected thermodynamic equilibrium speciation of carbon should be simple, as illustrated in Figure 22.4a at 600 °C and 5.0 kb. It can be seen that equilibrium between  $\text{CH}_4$ ,  $\text{CO}_2$ ,  $\text{HCO}_3^-$ , and  $\text{CO}_3^{2-}$  is depicted. No aqueous ionic C-species with intermediate oxidation states have predominance fields on the diagram. In contrast, it can be seen in Figure 22.4b that consideration of acetic acid and acetate at 600 °C and the much higher pressure of 50 kb results in the prediction of a substantial predominance field for acetate and a very small one for acetic acid

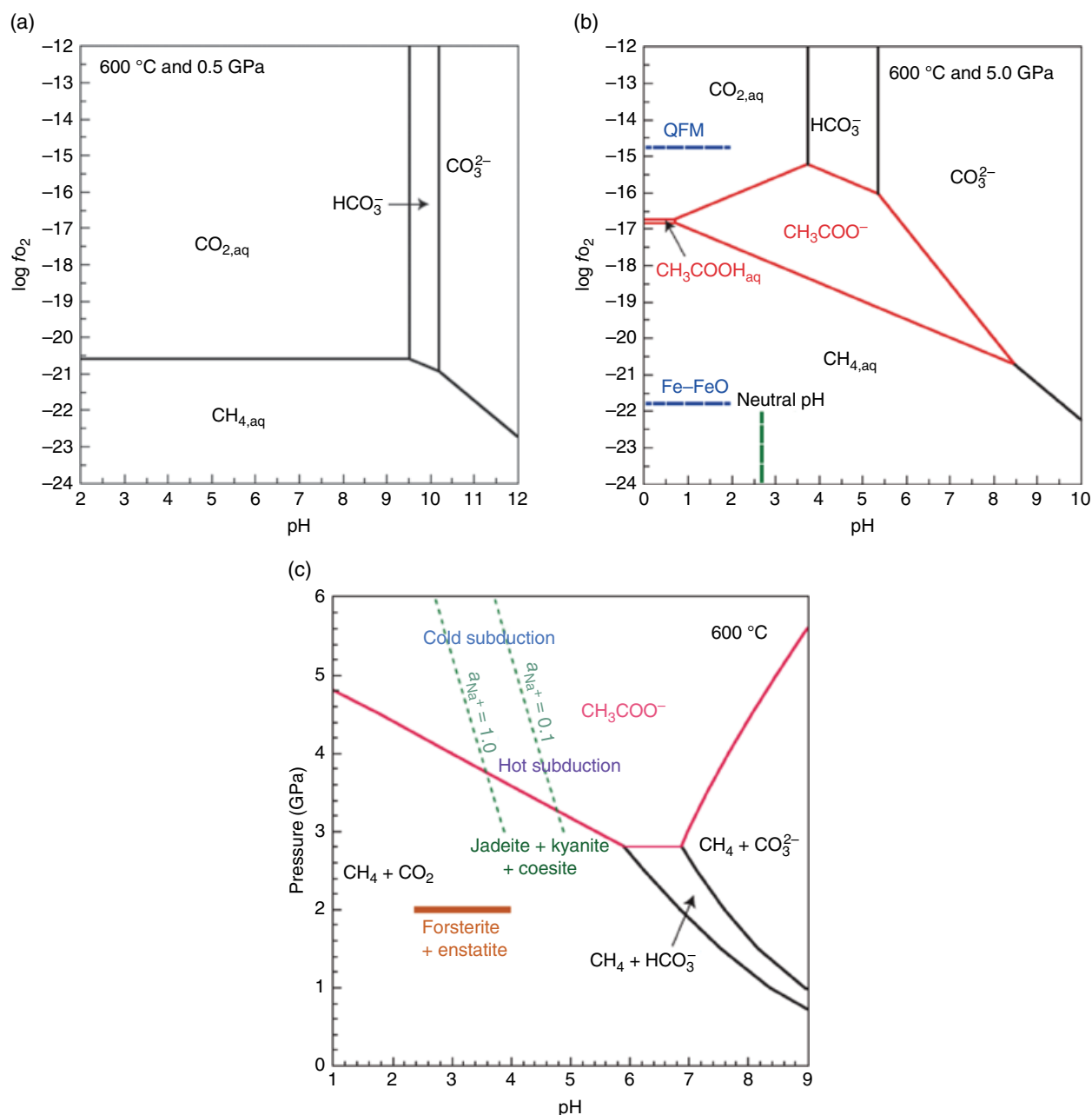


**Figure 22.4** Predicted aqueous C-speciation at 600 °C (Sverjensky, Stagno, et al., 2014). (a) Low pressure. (b) High pressure. (c) Predicted aqueous C-speciation as a function of pressure and pH. Expected pH ranges are shown for forsterite+enstatite (peridotite) and jadeite+kyanite+coesite (metasedimentary eclogite). See electronic version for color representation of the figures in this book.

(Sverjensky, Stagno, et al., 2014). Calculations such as these, using the DEW model, give a different picture of C-speciation in upper mantle fluids to that offered by the COH fluid model. More generally, it is predicted that in upper mantle fluids there is the possibility of a thermodynamically stable, rich variety of aqueous C-species with a wide range of oxidation states of carbon between those of carbon in  $CH_4$  and  $CO_2$ . Furthermore, all the C-species are thermodynamically linked to the major element

compositions of the silicate rocks. The richness of the aqueous organic C-speciation in upper mantle fluids is analogous to that in the shallow crust. The major difference, however, is that at upper mantle pressures there is complete thermodynamic equilibrium between all the aqueous C-species, including  $CH_4$ , whereas in shallow crustal fluids metastable equilibria exists.

It is clear from Figures 22.4 a and b that fluids at 50.0 kb are predicted to behave differently than fluids

at 5.0 kb. At what pressure does this transition take place? In the specific case of acetate, model calculations indicate the appearance of significant quantities of acetate relative to C(IV) species at about 29.0 kb at 600 °C, as shown in Figure 22.4c. At 800 °C, the transition pressure is predicted to be about 39.0 kb, and by 1000 °C there is no significant amount of acetate relative to oxidized C-species (Sverjensky, Stagno, et al.; 2014). It should be emphasized that the calculations reported in Figures 22.4 a–c considered only acetate and acetic acid as organic C-species. Other organic C-species, including metal-organic complexes, are likely to be more important (Huang & Sverjensky, 2019). Overall, these results indicate that thermodynamic equilibrium between all aqueous C-species, both inorganic and organic, is a strong function of the pressure of the fluid.

### 22.3.1.2. $\text{H}_2\text{CO}_3^0$ : The Forgotten Molecule in Upper Mantle Fluids

All the models discussed above have assumed that the predominant electrically neutral oxidized C-species in water is  $\text{CO}_2^0$ , as at ambient conditions. However, a theoretical ab initio molecular dynamics study of the  $\text{Na}_2\text{CO}_3 - \text{H}_2\text{O}$  system at conditions up to 727 °C and 10.0 GPa (Pan & Galli, 2016) revealed two surprising and very important results. First, a variety of  $\text{NaHCO}_3$  and  $\text{Na} - \text{CO}_3$  complexes dominate the aqueous C-speciation, and second,  $\text{H}_2\text{CO}_3^0$  is a much more abundant molecule than  $\text{CO}_2^0$ . The latter is the complete opposite to the situation under ambient conditions in water.

The discovery by ab initio molecular dynamics of the importance of  $\text{H}_2\text{CO}_3^0$  relative to the traditionally used  $\text{CO}_2^0$  in high pressure aqueous fluids made by Pan and Galli (2016) raises an important question. Under which conditions does the transformation takes place? Experimental determinations of the thermodynamic stability of  $\text{H}_2\text{CO}_3^0$  at near ambient conditions have long been reported (Soli & Byrne, 2002; Wissbrun et al., 1954). And in situ spectroscopic indications of the existence of  $\text{H}_2\text{CO}_3^0$  at low and high temperatures have been reported (Abramson et al., 2017; Dubessy et al., 1999; Lam et al., 2014). The trace amounts of  $\text{H}_2\text{CO}_3^0$  relative to  $\text{CO}_2^0$  in aqueous solutions at ambient conditions have made it convenient for geochemists to ignore the hydrate  $\text{H}_2\text{CO}_3^0$ . Under crustal hydrothermal and metamorphic conditions extending into the upper mantle, numerous studies of  $\text{CO}_2 - \text{H}_2\text{O}$  fluids exist using mixtures of the generic molecules  $\text{CO}_2$  and  $\text{H}_2\text{O}$  (e.g. Zhang & Duan, 2009). Quantifying the temperature and pressure conditions of the transformation of  $\text{CO}_2^0$  to  $\text{H}_2\text{CO}_3^0$  is important because it will potentially affect the modeling of all deep Earth fluids, as well as our understanding of carbon transport in the deep carbon cycle.

### 22.3.2. Experimental Studies

Recent experimental studies have started to test some of the predictions discussed above about aqueous C-species under upper mantle conditions. Specifically, the prediction that organic acid anions might be stable at pressures above about 30.0 kb in high-density fluids led to a diamond anvil cell study of the stability of Na-acetate solutions (Huang et al., 2017) at 300 °C and 30.0 kb. A very high concentration of Na-acetate (1.0 molal) was used to focus on acetate transformations. In situ analysis of the experimental products was made with Raman spectroscopy. Acetate was partly transformed into bicarbonate, and the bicarbonate to acetate ratio reached a steady state that persisted for the whole experiment, up to about 60 hours. However, the most dramatic result of the experiment was not predicted. Within a couple of hours of reaching the peak temperature and pressure in the experiments, it was discovered that immiscible isobutane fluid formed along with  $\text{CH}_4$  and  $\text{HCO}_3^-$  and eventually appeared to reach a steady state, coexisting with aqueous acetate and Na-carbonate crystals (Figure 22.5 a, b). The immiscibility could not be predicted, owing to a lack of adequate thermodynamic characterization at high pressures of even simple hydrocarbon fluids such as isobutane.

The results shown in Figures 22.5 a and b are also of interest because at 30 kb,  $\text{CH}_4$  formed easily and rapidly in the experiments, even at a temperature as low as 300 °C. This behavior contrasts sharply with Figure 22.3, according to which, at crustal pressures,  $\text{CH}_4$  formation will be kinetically hindered at 300 °C. Consequently, it appears that high pressure facilitates the formation of  $\text{CH}_4$  even at only 300 °C. In order to gain a more fundamental understanding of the kinetics of methane formation and the conditions under which immiscibility might occur, it will be essential to do more experiments and to develop theoretical models that will enable extrapolations to different temperatures and pressures and chemically more complex systems relevant to nature.

Immiscible behavior of hydrocarbon fluids was also discovered in another recent experimental study using synthetic fluid inclusions trapped in quartz (Li, 2017). An initial fluid consisting of 3 wt % NaCl and 18.5 wt%  $\text{HCOOH}$  in 78.5 wt %  $\text{H}_2\text{O}$  was buffered over a range of different oxidation states from Fe-FeO to Re- $\text{ReO}_2$  at 600 °C and 700 °C and 15.0 to 25.0 kb. The synthetic fluid inclusions showed evidence of trapping two immiscible fluids, one aqueous and one methane rich, denoted Type 1 and Type 2 in Figures 22.5 c and d. Other organic compounds were detected in both types of fluid inclusions, and  $\text{H}_2$  was also detected in methane-rich fluid inclusions from the most reducing conditions (i.e. with the Fe-FeO buffer). A remaining uncertainty for the latter inclusions

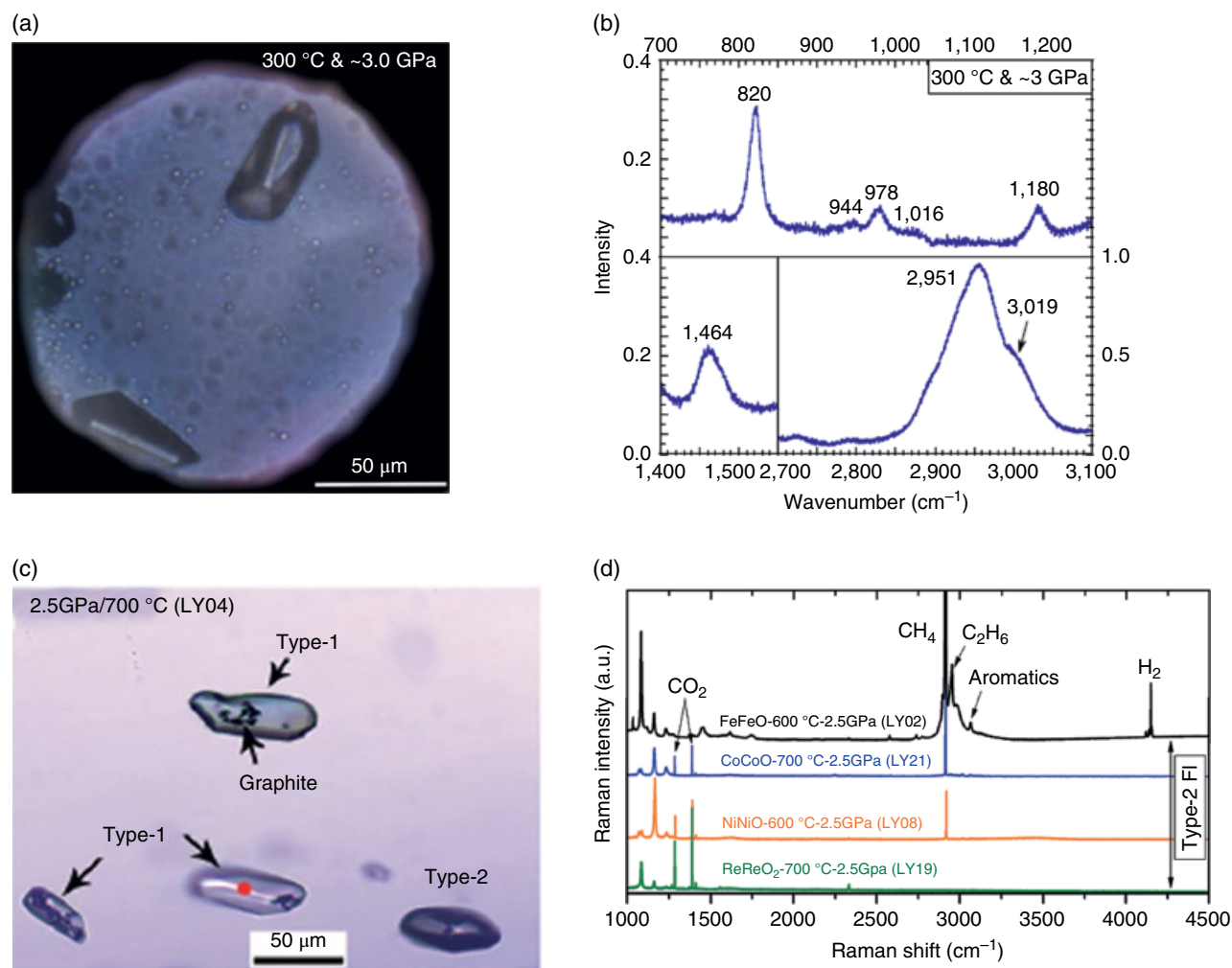


**Figure 22.5** Experimental evidence for immiscible hydrocarbon fluids. (a) Immiscible isobutane and aqueous fluid plus Na-carbonate crystals. (b) Raman spectrum of immiscible isobutane fluid (Huang et al., 2017). (c) Synthetic fluid inclusions in quartz showing two immiscible fluids. (d) Raman spectra (Li, 2017). See electronic version for color representation of the figures in this book.

is the nature of the methane-rich fluid at the elevated temperatures of trapping in quartz. It was clearly a hydrocarbon fluid, but it may have been a different hydrocarbon fluid before cooling to room temperature. It should be noted, however, that the experimental results shown in Figures 22.5 a–d refer to two different starting materials, Na-acetate and formic acid, as well as to very different temperatures and experimental durations that could have allowed the immiscible fluids to behave differently in the fluid inclusions. Nevertheless, both resulted in immiscibility between aqueous fluids and hydrocarbon fluids.

### 22.3.3. Field Studies

Immiscible hydrocarbon-rich fluids have now been documented in high-pressure metamorphic rocks. The

Lanzo massif in the Italian Western Alps is an example of an exhumed segment of high-pressure subducted oceanic lithosphere. The massif includes carbonated ultramafic rocks bearing hydrocarbon-rich fluid inclusions (Vitale Brovarone et al., 2017). Microstructures and stable isotope data constrained the genesis of the hydrocarbons to high-pressure events of fluid-rock interactions leading to a reduction of subducted carbonate minerals. In these rocks, two clearly different yet microstructurally coexisting fluid populations can be observed (Figure 22.6a). One population is present as negative crystal-shaped to rounded inclusions and consists of a single phase  $\text{CH}_4 + \text{H}_2$  fluid at ambient conditions, as identified by Raman spectroscopy (Figure 22.6b). The second population consists of two-phase (liquid-gas) inclusions and contains  $\text{CH}_4 + \text{H}_2\text{O} + \text{H}_2$  at ambient conditions (Figure 22.6b). Figure 22.6a shows a trail of



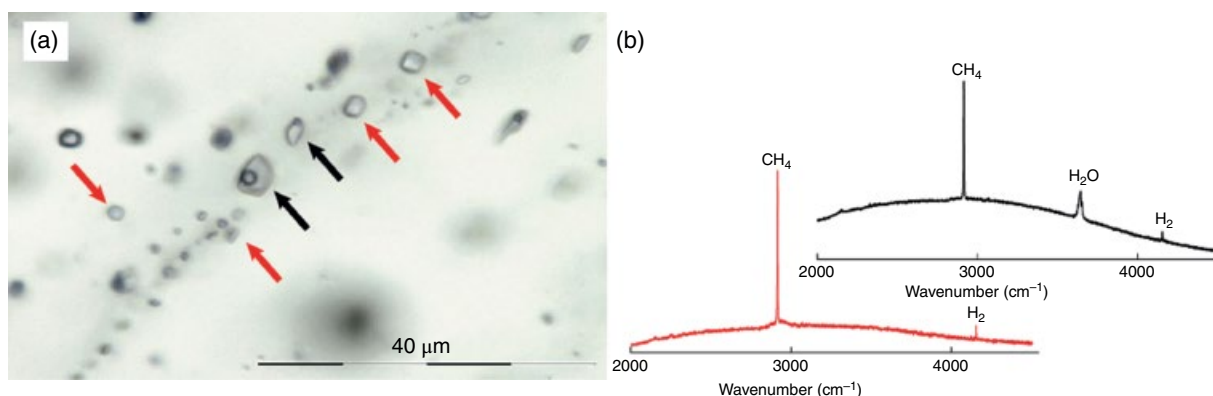


**Figure 22.6** Natural immiscible hydrocarbon and aqueous fluids in high-pressure rocks from the Lanzo massif, Italian Western Alps. (a) Fluid inclusions of two coexisting types. (b) Raman spectra of the two coexisting populations (Vitale Brovarone et al., 2017). See electronic version for color representation of the figures in this book.

pseudosecondary fluid inclusions containing both populations. The microstructure shows that the two fluids were both present during the trail formation, a strong indication of fluid immiscibility. Mineralogical features suggest that the formation and entrapment of these fluids happened at conditions of  $\leq 400$  °C and 1.0 GPa (Vitale Brovarone et al., 2017).

Documentation of natural high-pressure immiscible hydrocarbons is still scarce. The identification of natural immiscible hydrocarbons in the rock record, the quantification of the parameters controlling the immiscibility, and the definition of specific immiscible phases are hampered by two main features. The first one is the post-entrapment mechanical reworking of the fluid inclusions, which can lead to partial or even selective loss of the initial fluid composition (Bakker & Jansen, 1994; Hall & Sterner, 1993). As an example, Bakker and Jansen (1994) demonstrated that preferential  $\text{H}_2\text{O}$  leakage can occur in  $\text{H}_2\text{O}$  -  $\text{CO}_2$  fluid inclusions along dislocations and planar defects in the host mineral. Slight compositional variations related to leakage may render the identification of coexisting immiscible fluids particularly challenging. Comparison between multiple samples might therefore be necessary, yet not always possible. The second one is the respeciation of the fluid inclusions during cooling and decompression from their formation conditions. Methane appears to be the most common hydrocarbon species present in fluid inclusions in high-pressure rocks and analyzed at ambient conditions (Arai et al., 2012; Herms et al., 2012; Shi et al., 2005; Song et al., 2009). However, it is possible that the  $\text{CH}_4$  present in these inclusions, or part of it, results from the respeciation of more complex hydrocarbon fluids. In the Lanzo case study, the effect of at least local respeciation is suggested by the presence of daughter graphite in some individual fluid inclusions (Vitale Brovarone et al., 2017), which clearly indicates carbon redistribution within the inclusion later

than their formation (Cesare, 1995). Nevertheless, the resemblance of the natural fluid inclusions with the experimental results from Li (2017) under reducing conditions is clear: immiscible C-O-H and C-H fluids coexisted at subduction zone conditions. From this perspective, modern thermodynamic tools represent a powerful means to estimate the original speciation of natural hydrocarbon-rich fluids at high-pressure conditions.

## 22.4. CONCLUDING REMARKS

First, we have emphasized the long-standing evidence of metastable equilibria among aqueous C-species with different oxidation states under shallow crustal conditions. A great variety of aqueous C-species can coexist in this way when methane is prevented from forming, or reacting, by sluggish kinetics. Outstanding examples of this behavior include the short-chain aliphatic acids in brines in sedimentary basins and the amino acid tryptophan in a mid-ocean ridge environment, as well as a growing number of experimental studies of hydrocarbons, alcohols, and alkenes under hydrothermal conditions.

Second, we describe emerging evidence for a very different behavior for aqueous C-species at higher temperatures and pressures. It has long been assumed that temperatures greater than about 500 °C facilitate the ease of formation of methane in aqueous fluids, so that complete thermodynamic equilibrium among C-species can exist. For example, at 600 °C and 5.0 kb, the expected speciation is very simple:  $\text{CH}_4$ ,  $\text{CO}_2$ ,  $\text{H}_2\text{CO}_3^0$ ,  $\text{HCO}_3^-$ , and  $\text{CO}_3^{2-}$ . In contrast, at 600 °C and at pressures greater than about 30.0 kb, additional organic aqueous C-species may become thermodynamically stable, e.g. aliphatic acid anions in particular. Consequently, at upper mantle temperatures and pressures, there could be a rich C-speciation present in fluids with a great variety of oxidation states of C between  $-IV$  and  $+IV$ .

Third, we summarize theoretical, experimental, and field evidence that immiscible hydrocarbon fluids may coexist with aqueous fluids at upper mantle temperatures and pressures. Hydrocarbon fluids in subduction zones could represent a new mode of carbon transport in the deep carbon cycle and influence the oxidation state of their environments.

## ACKNOWLEDGMENTS

The authors wish to thank their collaborators in the Deep Carbon Observatory for numerous ideas and suggestions, particularly Mark Ghiorso, Craig Manning, Sami Mikhail, Vincenzo Stagno, and Everett Shock. Financial support is acknowledged from the Deep Carbon Observatory (Daniel, Sverjensky), and NSF Awards EAR-1624325 and ACI-1550346 (Sverjensky), and ANR T-ERC grant, CNRS INSU-SYSTER and MIUR Rita Levi Montalcini (Vitale Brovarone).

## REFERENCES

- Abramson, E. H., Bollengier, O., & Brown, J. M. (2017). Water-carbon dioxide solid phase equilibria at pressures above 4 GPa. *Scientific Reports*, 7, 821.
- Arai, S., Ishimaru, S., & Mizukami, T. (2012). Methane and propane micro-inclusions in olivine in titanoclinohumite-bearing dunites from the Sanbagawa high-P metamorphic belt, Japan: Hydrocarbon activity in a subduction zone and Ti mobility. *Earth Planet. Sci. Lett.*, 353–354, 1–11.
- Bakker, R. J., and Jansen, J.B.H. (1994). A mechanism for preferential H<sub>2</sub>O leakage from fluid inclusions in quartz, based on TEM observations. *Contributions to Mineralogy and Petrology*, 116, 7–20.
- Cesare, B. (1995). Graphite precipitation in C-O-H fluid inclusions: Closed system compositional density changes, and thermobarometric implications. *Contributions to Mineralogy and Petrology*, 122, 25–33.
- Dubessy, J., Moissette, A., Bäkker, R. J., Frantz, J. D., & Zhang, Y.-G. (1999). High-temperature Raman spectroscopic study of H<sub>2</sub>O-CO<sub>2</sub>-CH<sub>4</sub> mixtures in synthetic fluid inclusions: First insights on molecular interactions and analytical implications. *European Journal of Mineralogy*, 23–32.
- Etiopie, G., Ifandi, E., Nazzari, M., Procesi, M., Tsikouras, B., Ventura, G., et al. (2018). Widespread abiotic methane in chromitites. *Scientific Reports*, 8, 8728.
- Etiopie, G., & Sherwood Lollar, B. (2013). Abiotic methane on Earth. *Reviews of Geophysics*, 51, 276–299.
- Facq, S., Daniel, I., Montagnac, G., Cardon, H., & Sverjensky, D. A. (2016). Carbon speciation in saline solutions in equilibrium with aragonite at high pressure. *Chemical Geology*, 431, 44–53.
- Facq, S., Daniel, I., & Sverjensky, D. A. (2014). *In situ* Raman study and thermodynamic model of aqueous carbonate speciation in equilibrium with aragonite under subduction zone conditions. *Geochim. Cosmochim. Acta*, 132, 375–390.
- Hall, D. L., & Sterner, S. M. (1993). Preferential water loss from synthetic fluid inclusions. *Contributions to Mineralogy and Petrology*, 114, 489–500.
- Hermes, P., John, T., Bakker, R. J., & Shenk, V. (2012). Evidence for channelized external fluid flow and element transfer in subducting slabs (Raspas Complex, Ecuador). *Chemical Geology*, 310, 79–96.
- Huang, F., Daniel, I., Cardon, H., Montagnac, G., & Sverjensky, D. A. (2017). Immiscible hydrocarbon fluids in the deep carbon cycle. *Nature Communications*, 8.
- Huang, F., & Sverjensky, D. A. (2019). Extended Deep Earth water model for predicting major element mantle metasomatism. *Geochimica et Cosmochimica Acta*, 254, 192–230.
- Lam, R. K., England, A. H., Sheardy, A. T., Shih, O., Smith, J. W., Rizzuto, A. M., et al. (2014). The hydration structure of aqueous carbonic acid from X-ray absorption spectroscopy. *Chem. Phys. Lett.*, 614, 282–286.
- Li, Y. (2017). Immiscible CHO fluids formed at subduction zone conditions. *Geochem. Perspect. Lett.*, 3, 12–21.
- Manning, C. E. (1994). The solubility of quartz in H<sub>2</sub>O in the lower crust and upper-mantle. *Geochim. Cosmochim. Acta*, 58, 4831–4839.
- Manning, C. E. (2004). The chemistry of subduction-zone fluids. *Earth Planet. Sci. Lett.* 223, 1–16.
- Manning, C. E. (2018). Fluids of the lower crust: Deep is different. *Annu. Rev. Earth Planet. Sci.*, 46, 67–97.
- Manning, C. E., Shock, E. L., & Sverjensky, D. A. (2013). The chemistry of carbon in aqueous fluids at crustal and upper-mantle conditions: Experimental and theoretical constraints. *Reviews in Mineralogy and Geochemistry*, 75, 108–148.
- McCullom, T. M. (2013). Laboratory simulations of abiotic hydrocarbon formation in Earth's deep subsurface. *Rev. Mineral Geochem.*, 75, 467–494.
- McCullom, T. M., & Seewald, J. S. (2003a). Experimental constraints on the hydrothermal reactivity of organic acids and acid anions: I. Formic acid and formate. *Geochim. Cosmochim. Acta*, 67, 3625–3644.
- McCullom, T. M., & Seewald, J. S. (2003b). Experimental study of the hydrothermal reactivity of organic acids and acid anions: II. Acetic acid, acetate, and valeric acid. *Geochim. Cosmochim. Acta*, 67, 3645–3664.
- McDermott, J. M., Seewald, J. S., German, C. R., & Sylva, S. P. (2015). Pathways for abiotic organic synthesis at submarine hydrothermal fields. *Proceedings of the National Academy of Sciences*, 112, 7668–7672.
- Ménez, B., Pisapia, C., Andreani, M., Jamme, F., Vanbellingen, Q. P., Brunelle, A., et al. (2018). Abiotic synthesis of amino acids in the recesses of the oceanic lithosphere. *Nature*, 564, 59–63.
- Mikhail, S., Barry, P. H., & Sverjensky, D. A. (2017). The relationship between mantle pH and the deep nitrogen cycle. *Geochim. Cosmochim. Acta*, 209, 149–160.
- Mikhail, S., & Sverjensky, D. A. (2014). Nitrogen speciation in upper mantle fluids and the origin of Earth's nitrogen-rich atmosphere. *Nat. Geosci.*, 7, 816–819.
- Navon, O. (1999). Diamond formation in the Earth's mantle. *Proceedings of the 7th International Kimberlite Conference*. Cape Town: Red Roof Design, pp. 584–604.

- Pan, D., & Galli, G. A. (2016). The fate of carbon dioxide in water-rich fluids in the Earth's mantle. *Science Advances*, 2, e1601278–e1601278.
- Pan, D., Spanu, L., Harrison, B., Sverjensky, D. A., & Galli, G. (2013). The dielectric constant of water under extreme conditions and transport of carbonates in the deep Earth. *Proceedings of the National Academy of Sciences*, 110, 6646–6650.
- Shock, E. L. (1992). Chemical environments of submarine hydrothermal systems. *Orig Life Evol Biosph*, 22, 67–107.
- Scott, H. P., Hemley, R. J., Mao, H., Hershbach, D. R., Fried, L. E., Howard, W. M., & Bastea, S. (2004). Generation of methane in the Earth's mantle: In situ high pressure–temperature measurements of carbonate reduction. *Proc. Natl. Acad. Sci*, 101, 14023–14026.
- Seewald, J. S. (1994). Evidence for metastable equilibrium between hydrocarbons under hydrothermal conditions. *Nature*, 370, 285–287.
- Seewald, J. S., Zolotov, M., & McCollom, T. M. (2006). Experimental investigation of single carbon compounds under hydrothermal conditions. *Geochim. Cosmochim. Acta*, 70, 446–460.
- Shi, G. U., Tropper, P., Cui, W., Tan, J., & Wang, C. (2005). Methane (CH<sub>4</sub>)-bearing fluid inclusions in the Myanmar jadeitite. *Geochemical Journal*, 39, 503–516.
- Shipp, J., Gould, I. R., Herckes, P., Shock, E. L., Williams, L. B., & Hartnett, H. E. (2013). Organic functional group transformations in water at elevated temperature and pressure: Reversibility, reactivity, and mechanisms. *Geochim. Cosmochim. Acta*, 104, 194–209.
- Shirey, S. B., Cartigny, P., Frost, D. J., Keshav, S., Nestola, F., Nimis, P., et al. (2013). Diamonds and the geology of mantle carbon. *Rev Mineral Geochem*, 75, 355–421.
- Shock, E. L. (1988). Organic acid metastability in sedimentary basins. *Geology*, 16, 886–890.
- Shock, E. L. (1990). Geochemical constraints on the origin of organic compounds in hydrothermal systems. *Origins of Life and the Evolution of the Biosphere*, 20, 331–367.
- Shock, E. L., & Canovas, P. (2010). The potential for abiotic organic synthesis and biosynthesis at seafloor hydrothermal systems. *Geofluids*, 10, 161–192.
- Shock, E. L., Canovas, P., Yang, Z., Boyer, G., Johnson, K., Robinson, K., et al. (2013). Thermodynamics of organic transformations in hydrothermal fluids. *Reviews in Mineralogy and Geochemistry*, 76, 311–350.
- Soli, A. L., & Byrne, R. H. (2002). CO<sub>2</sub> system hydration and dehydration kinetics and the equilibrium CO<sub>2</sub>/H<sub>2</sub>CO<sub>3</sub> ratio in aqueous NaCl solution. *Mar. Chem.*, 78, 65–73.
- Song, S., Su, L., Niu, Y., Lai, Y., & Zhang, L. (2009). CH<sub>4</sub> inclusions in orogenic harzburgite: Evidence for reduced slab fluids and implication for redox melting in mantle wedge. *Geochim. Cosmochim. Acta*, 73, 1737–1754.
- Sverjensky, D. A., Harrison, B., & Azzolini, D. (2014). Water in the deep Earth: The dielectric constant and the solubilities of quartz and corundum to 60 kb and 1,200 °C. *Geochim. et Cosmochim. Acta*, 129, 125–145.
- Sverjensky, D. A., Stagno, V., & Huang, F. (2014). Important role for organic carbon in subduction-zone fluids in the deep carbon cycle. *Nat. Geosci.*, 7, 909–913.
- Tropper, P., & Manning, C. E. (2007). The solubility of corundum in H<sub>2</sub>O at high pressure and temperature and its implications for Al mobility in the deep crust and upper mantle. *Chemical Geology*, 240, 54–60.
- Vitale Brovarone, A., Martinez, I., Elmaleh, A., Compagnoni, R., Chaduteau, C., Ferraris, C., & Esteve, I. (2017). Massive production of abiotic methane during subduction evidenced in metamorphosed ophiocarbonates from the Italian Alps. *Nature Communications*, 8, 14134.
- Wissbrun, K. F., French, D. M., & Patterson Jr, A. (1954). The true ionization constant of carbonic acid in aqueous solution from 5 to 45. *The Journal of Physical Chemistry*, 58, 693–695.
- Yang, Z., Gould, I. R., Williams, L. B., Hartnett, H. E., & Shock, E. L. (2012). The central role of ketones in reversible and irreversible hydrothermal organic functional group transformations. *Geochim. Cosmochim. Acta*, 98, 48–65.
- Zhang, C., & Duan, Z. (2009). A model for C-O-H fluid in the Earth's mantle. *Geochim. Cosmochim. Acta*, 73, 2089–2102.